

Validity of the one-dimensional dissipative Boltzmann equation for point particles up to the clustering regime

José Miguel Pasini* and Patricio Cordero†

Departamento de Física, Facultad de Ciencias Físicas y Matemáticas, Universidad de Chile, Santiago, Chile

(Dated: December 22, 2018)

We study stationary states of a one-dimensional gas of point-like particles not subject to gravity between two walls at temperatures T_- and T_+ , with $T_- < T_+$. Depending on the normalized temperature difference $\Delta = (T_+ - T_-)/(T_+ + T_-)$ the system may be completely fluidized, or in a mixed state in which a cluster coexists with the fluidized gas. We devise and explain in detail a method for integrating the one-dimensional dissipative Boltzmann equation in the test-particle limit for the stationary case. We then apply this method to test the equation's validity up to the clustering regime, by comparing with results from microscopic Newtonian molecular dynamics. There is very good agreement, with the one-particle phase space density function presenting highly non-Gaussian features, and a discontinuity that corresponds to the test-particle limit. We conclude that Boltzmann's equation is valid at least everywhere in the control parameter space where the system has no cluster. The behavior of the system in its fluid phase is dominated by characteristic lines which resemble trajectories of particles subjected to a force which attracts them to a fixed point. If this point is in the physical region a cluster forms, if not then the system remains fluid.

PACS numbers: 45.70.-n, 05.20.Dd, 02.60.Cb, 02.70.-c

I. INTRODUCTION

Granular systems have been the focus of much attention due both to the theoretical challenges they present [1] and to the applications of industrial importance that stem from the rich phenomena they exhibit (see Refs. [1, 2, 3] and references therein). These systems are characterized by an energy loss in collisions, and this loss is at the base of many interesting phenomena. Among these, the clustering of particles has drawn much attention [4, 5, 6, 7].

In this paper we study in detail the mechanisms that dominate the collective dynamics of a one-dimensional system of point-like particles that interact via collisions that conserve momentum but dissipate kinetic energy. A cluster may or may not form. The system is confined in a box of unit length and any particle that reaches a wall is expelled from it with its velocity randomly chosen so that the velocity distribution of “outgoing” particles is a Maxwellian distribution with the “temperature” of that wall. There are no external forces. In a previous article [7] we saw that there are two relevant control parameters: the restitution coefficient which characterizes the collisions and the normalized temperature difference Δ between the walls, $\Delta = \frac{T_+ - T_-}{T_+ + T_-}$. In the plane of these two parameters there is a *transition line*: on one side the system is a granular fluid that reaches a stationary regime while in the other side a cluster is formed and, apparently, no stationary solution can be reached, at least in the limit of infinitely many particles. In Ref. [7] we

described what happens, while in the present paper we disclose the underlying mechanisms.

Two aspects have to be distinguished. On the one hand there is the formal aspect: we show that Boltzmann's equation describes closely what we get from molecular dynamic simulations in the case of the pure fluid phase even quite close to the transition line. On the other, there is an intuitive picture—originated in our detailed integration of Boltzmann's equation described in this paper—that we explain in the following paragraphs.

To fix notation, if c_1 and c_2 are the velocities of two particles that are about to collide, their velocities after the collision are given by

$$c'_1 = qc_1 + (1 - q)c_2, \quad c'_2 = (1 - q)c_1 + qc_2.$$

Here $q = (1 - r)/2$, where r is the usual restitution coefficient. For the elastic case ($r = 1$) the particles simply exchange velocities. Since the grains are point-like, the elastic case is then indistinguishable from a system in which the particles do not interact. To make this more explicit, the point-like character of the grains allows us to exchange their identities after the collision, giving the collision rules

$$c'_2 = qc_1 + (1 - q)c_2, \quad c'_1 = (1 - q)c_1 + qc_2.$$

Thus, when $q = 0$ the velocities are unaffected, and when q is small the velocities are only barely changed. This leaves us with the picture of a system of weakly interacting particles, whose relative velocity diminishes upon collisions.

The one dimensional granular system is being excited from the two walls, generally at different temperatures, T_- and T_+ . Particles emerging from the walls act as an outcoming “wind” pushing the particles away from them. One could picture the effect of this wind as an effective

*jmp84@cornell.edu; Present address: Department of Theoretical and Applied Mechanics, Cornell University, Ithaca, NY 14853, USA

†<http://www.cec.uchile.cl/cinetica/>

repulsive force which pushes the particles away from the walls. If the temperature difference between the two walls is large enough, the repulsive force associated to the hotter wall prevails over the force associated to the colder wall all across the system. Therefore in this case the overall effect is a net force always pointing toward the colder wall, much like gravity acts in a gas, always pointing to the base. If, on the contrary, the temperature difference is not large enough, there is a point in the system where the two repulsive forces cancel each other, producing an equilibrium point—a particle at rest in this point would tend to remain at rest—about which a cluster will grow. As the cluster absorbs particles the density of the surrounding gas decreases, and the equilibrium point may shift in time.

The article is organized as follows. In Sec. II we state the kinetic equation in the limit which the authors of Ref. [8] call the *hydrodynamic limit* of the one-dimensional Boltzmann equation for point-like grains. This limit is analogous to the Boltzmann-Grad limit of infinitely many particles and finite mean free path. In the present case, the role of the inverse of the mean free path is played by the factor qN , where N is the number of particles, and q is the inelasticity factor mentioned above. This factor represents how much is the velocity of a fast test-particle affected by crossing the system, when the inelasticity q is very small [7, 9]. The boundary conditions and normalization used are also stated.

Section III focuses on the stationary state, and describes the algorithm devised for the kinetic equation in this case.

Section IV contains results and conclusions. It compares the distribution functions in the one-particle phase space $f(x, c)$ (where x is the spatial coordinate, and c is the velocity) with the same distribution measured from molecular dynamic simulations. The numerical solution presents a discontinuity that stems from the limit taken in Sec. II, which allows the equation to be treated as approximately linear. The measured distribution exhibits a softened version of the discontinuity that steepens as we consider systems with larger number of particles (thus approximating better the limit of Sec. II). An intuitive picture is finally put forward.

II. KINETIC EQUATION, BOUNDARY CONDITIONS, AND NORMALIZATION

In the limit $N \rightarrow \infty$, but keeping qN fixed, the one-dimensional Boltzmann equation transforms into the test-particle equation [5, 6, 8]:

$$\partial_t f + c \partial_x f = qN \partial_c (Mf), \quad (1)$$

where

$$M(x, c) = \int_{-\infty}^{\infty} f(x, c') (c - c') |c - c'| dc'. \quad (2)$$

Since the equation is nonlinear, we must define explicitly the normalization used. In this case it is

$$\int_0^1 \int_{-\infty}^{\infty} f(x, c) dc dx = 1. \quad (3)$$

The system is confined in a box of unit length, and the particles may have any velocity: $(x, c) \in [0, 1] \times (-\infty, \infty)$. Any particle that reaches a wall is instantaneously expelled from it—there is no adsorption—with its velocity randomly chosen so that the velocity distribution of expelled particles is a Gaussian distribution with the temperature of that wall. This corresponds to choosing a wall kernel without memory and without a delay time (see Ref. [10], for example):

$$f(0, c > 0) \propto e^{-c^2/2T_-} \quad f(1, c < 0) \propto e^{-c^2/2T_+}. \quad (4)$$

The temperatures at both walls are chosen so that the system temperature for the perfectly elastic case is $T_0 = \sqrt{T_- T_+} = 1$. We will always take $T_+ > T_-$.

The missing constants in Eq. (4) are determined by Eq. (3) and by imposing that there is no flow across the walls:

$$\int_{-\infty}^{\infty} c f(x_{\text{wall}}, c) dc = 0. \quad (5)$$

III. STATIONARY STATE: SOLUTION ALGORITHM

In a stationary situation, Eq. (1) may be rewritten as follows:

$$c \partial_x f - qNM \partial_c f = qN f \partial_c M. \quad (6)$$

The coefficient $-qNM$ multiplying $\partial_c f$ plays the role of a force (per unit mass) and it is what we have called *wind*, in the introduction. It is the effective total force on a particle at x with velocity c . When f is reasonably close to the true solution, M will not depend on the detailed form of the distribution. Thus, if we have a trial distribution f_n , we may consider M and $\partial M/\partial c$ as given functions of x and c , and then we may solve Eq. (6) for the distribution f_{n+1} . Seen in this light, when the trial function is reasonably close to the solution, Eq. (6) is approximately a linear partial differential equation that can be analyzed as a hyperbolic equation, using the notion of characteristic curves [11]. In the present case, the characteristic curves satisfy

$$\frac{dx}{ds} = c \quad (7)$$

$$\frac{dc}{ds} = -qNM(x, c) \quad (8)$$

$$\frac{df}{ds} = qN f \partial_c M(x, c), \quad (9)$$

where s is a parameter.

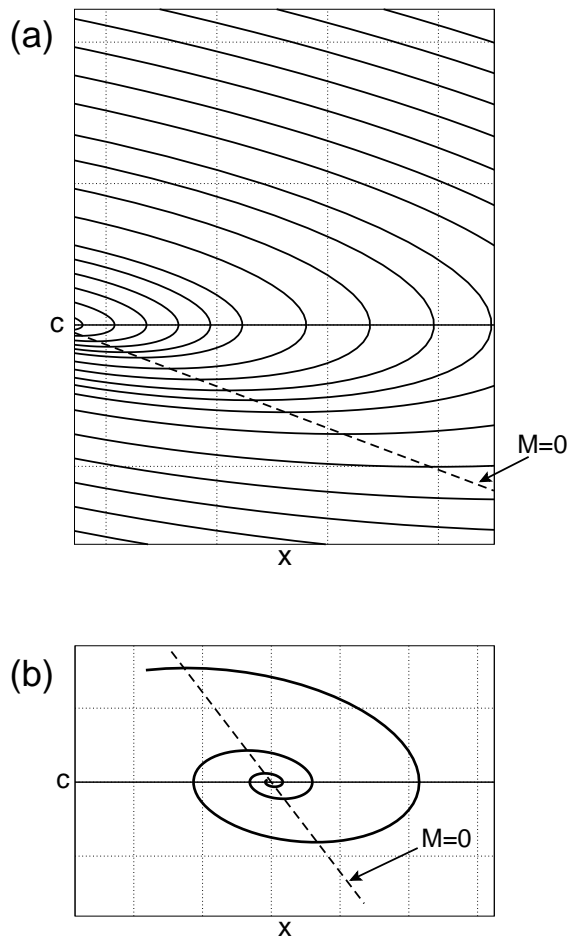


FIG. 1: Schematic representation of the form of the characteristic curves in (x, c) -space when the right wall is hotter than the left wall. Subfigure (a) shows the case where the curve $M(x, c) = 0$ does not cross the $c = 0$ line. Subfigure (b) shows how a characteristic curve would wind around the point where the $M = 0$ and $c = 0$ lines cross.

In simple words, our integro-differential equation is treated as if it were a (quasi-linear) partial differential equation and, since real characteristics exist, it is possible to integrate along these lines as if dealing with an ordinary differential equation with a single independent variable s .

Briefly put, given a distribution f_n (which implies that we have M_n and $\partial_c M_n$), we calculate f_{n+1} by solving

$$c \partial_x f_{n+1} - qNM_n \partial_c f_{n+1} = qN f_{n+1} \partial_c M_n \quad (10)$$

through numerical integration along the characteristics, following Ref. [12]. After the integration we normalize f_{n+1} to one, and then use f_{n+1} to calculate f_{n+2} . In this way we eventually reach a fixed point.

As will be described in detail in the following section, there are three types of characteristics: (1) those that originate at $x = 0$ with a large positive velocity and end at $x = 1$; (2) those that also begin at $x = 0$ (implying $c > 0$) but do not reach $x = 1$: they reach the $c = 0$ axis,

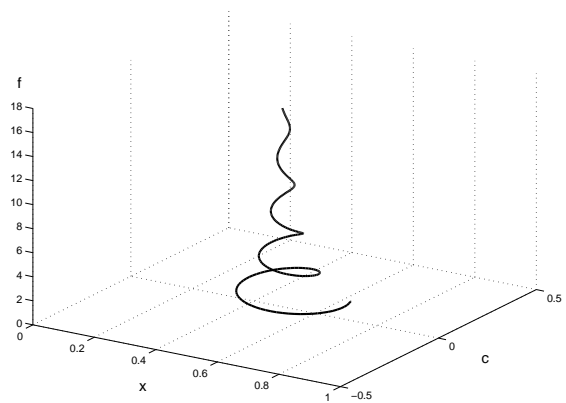


FIG. 2: Qualitative picture of the shape of a characteristic curve in (x, c, f) -space for the case where the $M = 0$ curve crosses the $c = 0$ line.

turn around, and return to $x = 0$; (3) those that start at $x = 1$ (implying $c < 0$) and end at $x = 0$. The first two types of characteristics are associated to the left boundary condition, while the third type is associated to the right boundary condition. The solution, therefore, may be discontinuous along the separatrix of these last two types of characteristics. Since our numerical algorithm integrates along these characteristics, it never crosses the discontinuity; every step deals with a smooth function.

As in Refs. [5, 6] we may consider that the projection of any characteristic line to the (x, c) plane corresponds to the phase-space trajectory of a *test particle* crossing the system. From Eq. (8) we confirm what has been said before, namely that $-qNM$ is the acceleration of the particle. For large velocities $M \sim c|c|$, hence if the particle's velocity is large it will be slowed down. This is suggested in Fig. 1(a), where the characteristics far from $c = 0$ approach that axis.

Due to the form of Eqs. (7) and (8), the intersection of the curves $c = 0$ and $M(x, c) = 0$ is interesting [13]. At $c = 0$ the characteristic curves in the (x, c) plane are vertical, and at $M = 0$ they are horizontal. Figure 1(b) is a sketch of what would happen to the characteristic curves around the intersection point (which we will call G henceforward): they would wind around it, never reaching it. Meanwhile, since $\partial_c M > 0$ in that vicinity, we have that f is increasing along the curve. In other words, in (x, c, f) -space the characteristic curve is practically vertical, with f increasing sharply along it. This case, depicted qualitatively in Fig. 2, corresponds to the presence of a cluster at the intersection point G .

Hence, for the system to be able to reach a stationary fluidized state, the curve $M = 0$ must never cross the c axis. In Fig. 1(a) we have drawn this curve in the lower part of the plane, which corresponds to the case when the left wall is the colder one ($T_- < T_+$) and the temperature difference is large enough that no cluster can form.

Further details of the algorithm are relayed to the appendix.

IV. RESULTS AND CONCLUSIONS

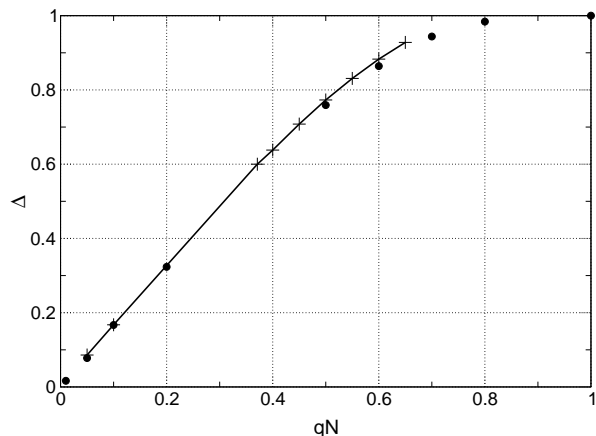


FIG. 3: Comparison between the threshold for cluster formation in molecular dynamics and the loss of convergence in the algorithm. The plus signs show the lowest values of Δ for each qN before the algorithm becomes unstable. The circles show the lowest values of Δ for each qN before a cluster is detected in a molecular dynamics simulation of $N = 1000$ particles. The plus signs are joined by lines to guide the eye.

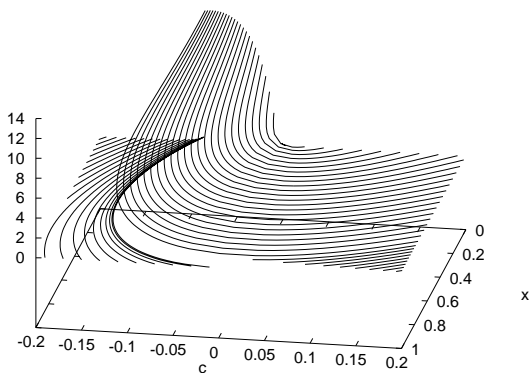


FIG. 4: Distribution function $f(x, c)$ for the case $qN = 0.35$ and $\Delta = 0.6$. Only one every four curves is shown to unclutter the picture.

Figure 3 shows the threshold for cluster formation in molecular dynamics and the loss of convergence in the algorithm. We can say that they coincide, namely, the integration of Boltzmann's equation with the present algorithm converges almost to the transition line beyond which a cluster begins to form.

Figure 4 shows the characteristic lines in (x, c, f) -space when $qN = 0.35$ and $\Delta = 0.6$. Although it corresponds to a completely fluidized case it is not too far from the transition line, as can be seen in Fig. 3.

Figure 5 shows the projection of the characteristic

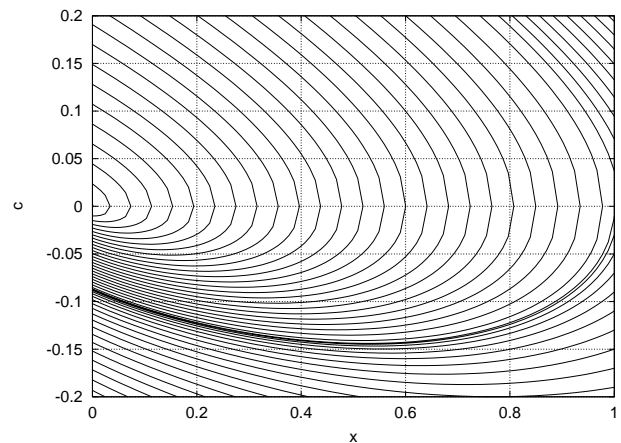


FIG. 5: Projection of the characteristic curves into (x, c) -space for the same case as Fig. 4. Only one every four curves is shown to unclutter the picture.

curves into the (x, c) plane. The asymmetric aspect of the family of curves is due to the effective force which pushes particles toward the colder wall almost as if there was a space-dependent gravity-like force. The figure only shows the characteristic lines for small values of the velocity since further away the distribution is a bimodal Gaussian. One interesting feature of this figure is the density of lines near $x = 0$ for small negative velocity. It corresponds to a remarkable peak of the velocity distribution for velocities much smaller than the thermal velocity. In the present case the thermal velocity for the particles approaching the wall is about $\sqrt{2}$, an order of magnitude larger than the width of the peak.

To check how the distribution obtained from our algorithm compares with the distribution stemming from molecular dynamic simulations we show the distribution at the colder wall $f(0, c)$, where the discontinuity is more notorious. In Fig. 6 we compare with molecular dynamic results for $N = 1000$ particles, $qN = 0.1$, and $\Delta = 0.6$, namely quite far from the clustering regime. Figure 6(a) shows the distribution for a wide range of velocities (at this scale the calculated and the simulated solutions cannot be resolved by the naked eye). It can be checked that the distribution behaves as two Maxwellians, one for $c > 0$ and a different one for $c < 0$ (with $|c|$ sufficiently large), and has a remarkable peak for small negative velocities. Even though the system is far from the clustering regime, that peak is a reminder that a clustering singularity exists.

Figure 6(b) shows in detail the shape of the discontinuous behavior at the peak. The discontinuity that the analytic analysis predicts is softened in the simulations. This difference is due to size effects. In fact, as seen in Fig. 7 (which corresponds to a system on the verge of clusterization), simulations of systems with an increasing number of grains exhibit increasingly steeper behavior at the predicted discontinuity, approaching the result that Boltzmann's equation implies and our algorithm yields.

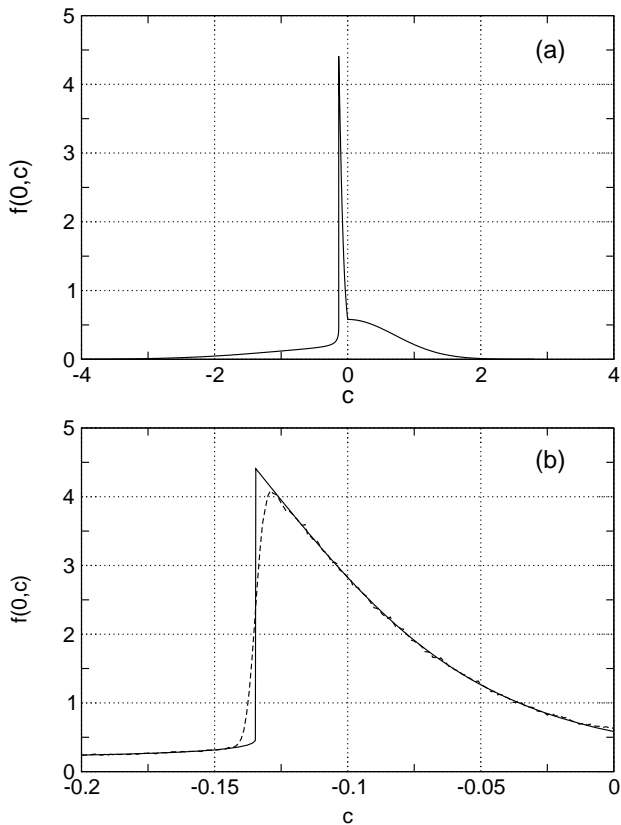


FIG. 6: Distribution function at the cold wall for the case $qN = 0.1$ and $\Delta = 0.6$. The solid curve results from applying the algorithm described in the text, while the dashed curve was measured from a molecular dynamics simulation with $N = 1000$ particles. Subfigures (a) and (b) show the same data, but on a different scale. Subfigure (a) emphasizes how the distribution is essentially Gaussian, save for the sharp peak for slow particles. Subfigure (b) shows a detail of this peak, showing how the discontinuity is smoothed in the simulation.

The final picture that emerges from all that has been said is, first, that Boltzmann's equation for the quasi-elastic system is valid essentially in all points of the (q, Δ) plane where the system has no cluster. The behavior of the system in its fluid phase is dominated by characteristic lines, trajectories of a *test particle* subjected to a force which attracts it to a point G where the $M = 0$ line crosses the c -axis. In the fluid phase such point G is beyond the physical box, particles hit the colder wall, forget their past and reenter the system.

We have not solved the time-dependent case when G is inside the box. In such case many trajectories in phase space will wind around G (as shown in Figs. 1(b) and 2), and the density at that point will tend to diverge, thus forming a cluster.

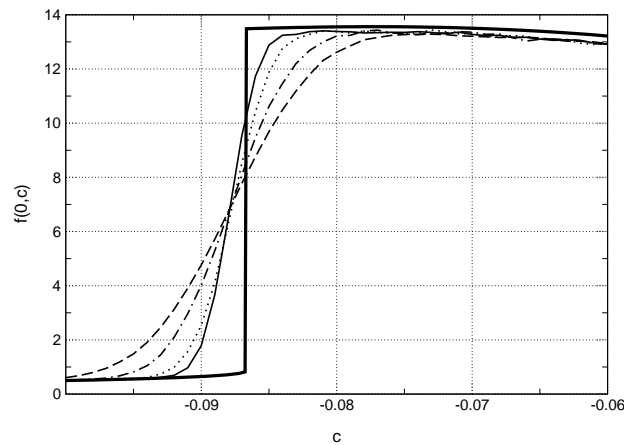


FIG. 7: Detail of the discontinuity in the distribution function at the left wall for $qN = 0.35$ and $\Delta = 0.6$. The thick solid line results of applying the algorithm described in the text. The other curves stem from molecular dynamics for 1000 (dashed), 2000 (dash-dotted), 5000 (dotted), and 10000 (thin solid line) particles.

Acknowledgments

This work has been partially funded by Fundación Andes, by *Fondecyt* grants No. 2990108 and No. 1000884, and by *Fondap* grant 11980002.

APPENDIX: ALGORITHM IN DETAIL

In order to commence the integration, we need some initial *ansatz* $f_0(x, c)$. This may be, for example, the solution for the elastic case:

$$f(x, c) = A \left\{ \theta(c) e^{-c^2/2T^-} + B[1 - \theta(c)] e^{-c^2/2T^+} \right\},$$

where $\theta(c)$ is the Heaviside step function, B is a constant chosen so as to have zero flux at the walls, and A is a normalization constant. In practice, if it is available, it is convenient to choose as f_0 a previous solution for a case similar to the one being studied. This not only speeds up the convergence, but also may help avoid the spurious appearance of G points at intermediate iterations.

The next step is to see whether the $M = 0$ curve crosses the $c = 0$ line. If it does, the algorithm breaks down, and we must start from a better *ansatz*. If it lies wholly on $c < 0$, the characteristic curves will behave qualitatively as in Fig. 1(a). In this case we start by integrating the characteristics that begin at $(x = 0, c > 0)$. If the curve lies wholly on $c > 0$ the situation is inverted, and we must start from $(x = 1, c < 0)$. In what follows we will assume that the situation is as in Fig. 1(a). This is always the case when we are sufficiently close to the solution.

The next step is finding the dividing characteristic. This is done directly by the bisection method, choosing different values of c_D so that the initial condition for the

characteristic is

$$x(s=0) = 0, \quad c(0) = c_D, \quad f_1(0) = A_- e^{-c_D^2/2T_-}.$$

The value of A_- is chosen so that the net flux at the wall is zero:

$$\int_{-\infty}^0 c f_0(0, c) dc + A_- \int_0^{\infty} c e^{-c^2/2T_-} dc = 0.$$

Integrating along this characteristic in very small steps we find c_D such that the corresponding curve has a turning point at $(x, c) = (1 - \epsilon, 0)$, with ϵ less than a reasonably small number.

With this value of c_D we divide the interval $0 < c < c_D$, choosing many values c_i (with $0 < c_1 < c_2 < \dots < c_D$) as starting points for characteristic curves. These will all be curves which will turn around and return to $x = 0$. The crossing points will define a natural discretization of the x axis which will be used to tabulate the values of f_1 . In this way we always sample the turning point.

Now we start the integration: with *increasing* i , we integrate the characteristic that starts with c_i , tabulating the values of $c(s)$ and $f(s)$ for values of x corresponding to the turning points of the previously integrated characteristics. This step is of paramount computational importance: at the next iteration we will need to calculate the integrals $M(x, c)$ and $\partial_c M(x, c)$. Since these are integrals in c keeping x fixed, it is important to have values

of $f(x, c)$ tabulated at the same values of x . This precaution allows us to evaluate M and $\partial_c M$ in a fast and straightforward manner.

Having integrated along all the characteristics with $c_i < c_D$, we now integrate characteristics that start from $(x = 0, c > c_D)$. These are curves that start at the left wall and reach the right wall, that is, they do not have a turning point. The completion of this step implies that we have f_1 in the whole half-space $c > 0$ (and also in part of $c < 0$).

At this point we can start integrating the characteristic curves that start at the right wall, choosing values of $c_0 < 0$:

$$x(s=0) = 1, \quad c(0) = c_0, \quad f_1(0) = A_+ e^{-c_0^2/2T_+}.$$

The value of A_+ is chosen so that the net flux at the wall is zero:

$$A_+ \int_{-\infty}^0 c e^{-c^2/2T_+} dc + \int_0^{\infty} c f_1(1, c) dc = 0.$$

After completing the integration, we normalize f_1 , and take the magnitude of this adjustment as a measure of how far we are from reaching a fixed point.

This procedure is repeated until a reasonable convergence is reached. Typically ten to fifteen iterations are necessary to achieve a good solution.

-
- [1] L. P. Kadanoff, Rev. Mod. Phys. **71**, 435 (1999).
 [2] H. M. Jaeger and S. R. Nagel, Science **255**, 1523 (1992).
 [3] H. M. Jaeger, S. R. Nagel, and R. P. Behringer, Physics Today **49** (4), 32 (1996).
 [4] S. McNamara and W. R. Young, Phys. Fluids A **4**, 496 (1992).
 [5] S. McNamara and W. R. Young, Phys. Fluids A **5**, 34 (1993).
 [6] E. L. Grossman and B. Roman, Phys. Fluids **8**, 3218 (1996).
 [7] J. M. Pasini and P. Cordero, Phys. Rev. E **63**, 041302 (2001).
 [8] R. Ramírez and P. Cordero, Phys. Rev. E **59**, 656 (1999).
 [9] Y. Du, H. Li, and L. P. Kadanoff, Phys. Rev. Lett. **74**, 1268 (1995).
 [10] C. Cercignani, *Mathematical Methods in Kinetic Theory* (Plenum Press, New York, 1990), 2nd ed.
 [11] R. Courant, *Methods of Mathematical Physics*, vol. 2 (Interscience, New York, 1962).
 [12] G. D. Smith, *Numerical Solution of Partial Differential Equations: Finite Difference Methods* (Clarendon Press, Oxford, 1984), 3rd ed.
 [13] Since $M \sim c|c|$ asymptotically, we can be sure that there is at least one $M = 0$ curve, and that if there is only one curve, then “above” it $M > 0$, and “below” it $M < 0$. Therefore in this case $\partial_c M > 0$ at the intersection of $M = 0$ and $c = 0$.